
Since January 2020 Elsevier has created a COVID-19 resource centre with free information in English and Mandarin on the novel coronavirus COVID-19. The COVID-19 resource centre is hosted on Elsevier Connect, the company's public news and information website.

Antiviral Research 201 (2022) 105297

Contents lists available at ScienceDirect

Antiviral Research

journal homepage: www.elsevier.com/locate/antiviral

# Isolation of human monoclonal antibodies with neutralizing activity to a broad spectrum of SARS-CoV-2 viruses including the Omicron variants

Mikako Ueno [a], Naoko Iwata-Yoshikawa [b], Akihiro Matsunaga [a], Tadashi Okamura [c], Sho Saito [d], Shinobu Ashida [d], Isao Yoshida [e], Mami Nagashima [e], Hiroyuki Asakura [e], Yuu Yaoita [e], Jun Suzuki [e], Kenji Sadamasu [e], Kazuhisa Yoshimura [e], Satoshi Kutsuna [d,f], Nozomi Shiwa-Sudo [b], Noriyo Nagata [b], Tadaki Suzuki [b], Akinori Suzuki [g], Miwa Okamoto [g], Moto Kimura [h], Norio Ohmagari [d], Ryu Miura [g,**], Yukihito Ishizaka [a,*]

[a] Department of Intractable Diseases, National Center for Global Health and Medicine, Tokyo, Japan
[b] Department of Pathology, National Institute of Infectious Diseases, Tokyo, Japan
[c] Department of Laboratory Animal Medicine, National Center for Global Health and Medicine, Tokyo, Japan
[d] Disease Control and Prevention Center, National Center for Global Health and Medicine, Tokyo, Japan
[e] Department of Microbiology, Tokyo Metropolitan Institute of Public Health, Tokyo, Japan
[f] Department of Infection Control, Graduate School of Medicine, Faculty of Medicine, Osaka University, Osaka, Japan
[g] Sapporo Laboratory, EVEC, Inc., Hokkaido, Japan
[h] Department of Academic-Industrial Partnerships Promotion, Center of Clinical Science, National Center for Global Health and Medicine, Tokyo, Japan

ARTICLE INFO

*Keywords:*
SARS-CoV-2
mAb
Spike protein
Neutralizing activity
Escape mutants
Omicron variants

ABSTRACT

Monoclonal antibody therapy is a promising option for severe acute respiratory syndrome coronavirus 2 (SARS-CoV-2) infection, and a cocktail of antibodies (REGN-COV) has been administered to infected patients with a favorable outcome. However, it is necessary to continue generating novel sets of monoclonal antibodies with neutralizing activity because viral variants can emerge that show resistance to the currently utilized antibodies. Here, we isolated a new cocktail of antibodies, EV053273 and EV053286, from peripheral blood mononuclear cells derived from convalescent patients infected with wild-type SARS-CoV-2. EV053273 exerted potent antiviral activity against the Wuhan wild-type virus as well as the Alpha and Delta variants *in vitro*, whereas the antiviral activity of EV053286 was moderate, but it had a wide-range of suppressive activity on the wild-type virus as well as the Alpha, Beta, Delta, Kappa, Omicron BA.1, and BA.2 variants. With the combined use of EV053273 and EV053286, we observed similar inhibitory effects on viral replication as with REGN-COV *in vitro*. We further assessed their activity *in vivo* by using a mouse model infected with a recently established viral strain with adopted infectious activity in mice. Independent experiments revealed that the combined use of EV053273 and EV053286 or the single use of each monoclonal antibody efficiently blocked infection *in vivo*. Together with data showing that these two monoclonal antibodies could neutralize REGN-COV escape variants and the Omicron variant, our findings suggest that the EV053273 and EV053286 monoclonal antibody cocktail is a novel clinically applicable therapeutic candidate for SARS-CoV-2 infection.

## 1. Introduction

### 1.1. Current therapeutic strategy against SARS-CoV-2

The pandemic of coronavirus disease 2019 (COVID-19) is caused by severe acute respiratory syndrome virus 2 (SARS-CoV-2, which emerged in Wuhan, China in late 2019. As of January 5, 2022, approximately 293 million individuals have been infected with SARS-CoV-2 and 5.45 million patients have died from COVID-19, with profound effects on social activity and human life (WHO, 2020; WHO Coronavirus).

* Corresponding author. Department of Intractable Diseases, National Center for Global Health and Medicine, Toyama 1-21-1, Shinjuku-ku, Tokyo, 162-8655, Japan.
** Corresponding author. Sapporo Laboratory, EVEC, Inc., Technopark 1-chome, Shimo-Nopporo, Atsubetsu-ku, Sapporo, Hokkaido, 004-0015, Japan.
*E-mail addresses:* r-miura@evec.jp (R. Miura), zakay@ri.ncgm.go.jp (Y. Ishizaka).

https://doi.org/10.1016/j.antiviral.2022.105297
Received 28 January 2022; Received in revised form 18 March 2022; Accepted 21 March 2022
Available online 24 March 2022

COVID-19 induces multi-organ failure and acute respiratory distress syndrome, which is caused by an excessive release of inflammatory mediators (i.e., a cytokine storm), resulting in lethal clinical outcomes (Kutsuna, 2020). Most patients with COVID-19 show seroconversion at 2 weeks after symptom onset, and the transfusion of plasma prepared from convalescent patients was tried initially as therapy (Kutsuna et al., 2020). Although monoclonal antibodies (mAbs) and small antiviral compounds such as remdesivir and molnupiravir (Fischer et al., 2022) have been approved by the U.S. Food and Drug Administration as therapeutic interventions, the pandemic is still ongoing, because new variants such as the Alpha, Delta, and Omicron strains have emerged as variants of concern.

### 1.2. mAbs against the spike protein of SARS-CoV-2

The application of mAbs against the spike (S) protein of SARS-CoV-2 is a promising approach to reduce virus copy number in patients and lower the risk of hospitalization. The receptor-binding domain (RBD) of the SARS-CoV-2 S-trimer is pivotal for binding to angiotensin converting enzyme 2 (ACE2), a host cell receptor, and the interaction of the RBD and ACE2 is a key target for neutralization. Potent RBD-specific antibodies have been isolated from many convalescent donors (Brouwer et al., 2020; Cao et al., 2020; Chen et al., 2020; Chi et al., 2020; Hansen et al., 2020; Ju et al., 2020; Robbiani et al., 2020; Rogers et al., 2020; Seydoux et al., 2020; Shi et al., 2020; Wec et al., 2020; Wu et al., 2020b; Zost et al., 2020), but it has been reported that RBD-specific neutralizing antibodies isolated during early convalescence have low levels of somatic hypermutations (Barnes et al., 2020b; Robbiani et al., 2020; Yuan et al., 2020), which accumulate in SARS-CoV-2 antibodies in the months after infection (Gaebler et al., 2021; Sakharkar et al., 2021; Sokal et al., 2021), resulting in greater neutralization potency with breadth and resilience to viral escape mutations (Moriyama et al., 2021; Muecksch et al., 2021b).

### 1.3. Combined use of mAbs is a standard clinical option

Among the mAbs used for the treatment of SARS-CoV-2 infection, REGN-COV effectively reduces viral titers and the rate of admission to healthcare units (Chen et al., 2021; Weinreich et al., 2021). REGN-COV comprises two distinct mAbs, casirivimab and imdevimab, because it was suspected that SARS-CoV-2, similar to other SARS-CoVs, could easily generate escape mutants. Actually, a clinical trial with the single use of a mAb for respiratory syncytial virus failed due to the emergence of escape mutants (Starr et al., 2021b). Additionally, bamlanivimab (also known as LY-CoV555) was applied to a clinical trial of SARS-CoV-2 patients and clinical outcome was compared with that of combined treatment of bamlanivimab with etesevimab, another mAb (Gottlieb et al., 2021). Although both monotherapy and combination therapy significantly reduced viral load, bamlanivimab-resistant mutant variants were detected in patients who received monotherapy, whereas no such variants were detected with combination therapy. These observations suggest that combination therapy with mAbs might be a standard strategy for mAb-based therapy. Notably, it was recently announced that REGN-COV does not show neutralizing activity to the Omicron variant (VanBlargan et al., 2022), also implying that it is necessary to continue searching for additional mAbs that can block a wide range of variant viruses.

### 1.4. Identification of a novel set of mAbs protecting against REGN-COV escape mutants

Here, we isolated several mAbs from convalescent patients and characterized the therapeutic potential of EV053273 and EV053286, the combined use of which appeared to be quite effective. These mAbs had distinct antiviral characteristics; EV053273 had remarkably potent neutralizing activity restricted to the wild-type virus well as the Alpha and Delta strains. In contrast, EV053286 had moderate neutralizing activity, but was effective against a wide range of viruses including the Omicron variant. Together with data showing that these mAbs could neutralize REGN-COV escape mutants, our findings suggest that the combination of EV053273 and EV053286 is an option for mAb therapy.

## 2. Materials and methods

### 2.1. Cells and viruses

VeroE6/TMPRSS2 cells were acquired from the Japanese Collection of Research Bioresources Cell Bank (National Institute of Biomedical Innovation, Health, and Nutrition, Osaka, Japan). They were cultured in Dulbecco's modified Eagle medium containing 10% fetal bovine serum (FBS) supplemented with 50 U/mL penicillin-streptomycin (Thermo Fisher Scientific) and 1 mg/mL G418 disulfate (Nacalai Tesque, Inc.). Wild-type SARS-CoV-2 hCoV-19/Japan/TY/WK-521/2020 (Wuhan lineage) EPI_ISL_408667 as well as mutant SARS-CoV-2 hCoV-19/Japan/QK002/2020 (Alpha variant) EPI_ISL_768526, hCoV-19/Japan/TY8-612-P1/2021 (Beta variant) EPI_ISL_1123289, and hCoV-19/Japan/TY7-501/2021 (Gamma variant) EPI_ISL_833366 strains were acquired from the National Institute of Infectious Diseases. hCoV-19/Japan/TKYTK1734/2021 (Delta variant) EPI_ISL_2378732, hCoV-19/Japan/TKYTK5356/2021 (Kappa variant) EPI_ISL_2378733, hCoV-19/Japan/TKYX00012/2021 (Omicron variant BA.1) EPI_ISL_8559478, and hCoV-19/Japan/TKYS02037/2022 (Omicron variant BA.2) EPI_ISL_9397331 strains were isolated under approval from the Institutional Review Board of the Tokyo Metropolitan Institute of Public Health, according to the 2013 amendment to the Declaration of Helsinki (acceptance number: 3KenKenKen-466). Briefly, VeroE6/TMPRSS2 cells were inoculated with 100 μL of nasopharyngeal swab in a biosafety level 3 laboratory. After incubation at 37 °C for 15 min, a maintenance medium consisting of Eagle minimum essential medium (056–08385; Fujifilm Wako Pure Chemical Corporation) supplemented with 2% FBS (Biowest) and 1% penicillin-streptomycin solution (5,000 IU/mL; MP Biomedicals) was added, and then cultured at 37 °C under 5% CO2. After confirming the cytopathic effect under an inverted microscope (Nikon), the viral titer of the culture supernatant was estimated by quantitative reverse transcription polymerase chain reaction (qRT-PCR) analysis. RNA was extracted from each virus strain using a QIAamp Viral RNA Mini Kit (Qiagen). Libraries were made using an NEBNext Ultra RNA Library Prep Kit for Illumina (E7530; New England BioLabs) and whole genome sequencing was performed with the MiSeq system (Illumina)

### 2.2. SARS-CoV-2 neutralization assay

Each antibody solution of EV053273, EV053286, cocktail (EV053273+EV053286), and REGN-COV (REG10933+REG10987) was serially diluted 2-fold in Opti-MEM (Thermo Fisher Scientific) and incubated with 100 median tissue culture infectious dose (TCID50) of SARS-CoV-2 for 1 h at 37 °C. Then, each mixture was added to VeroE6/TMPRSS2 cells, which had been plated at $1.0 \times 10^4$ cells/well in a 96-well plate with Dulbecco's modified Eagle medium containing 4% FBS at 1 day before viral infection. After 3 days (wild-type virus and Alpha, Beta, Gamma, Delta, and Kappa variants) or 4 days (Omicron variants BA.1 and BA.2), the cytopathic effect was semi-quantified using Cell Counting Kit-8 (Dojindo). The absorbance of each well was measured at 450 nm by using a microplate reader (Bio-Rad). The half-maximal inhibitory concentration (IC50) values of the neutralizing antibodies were calculated. The copy number of the culture supernatant was estimated by qRT-PCR using a SARS-CoV-2 Detection Kit -N2 set- (Toyobo) with the StepOnePlus Real-Time PCR System (Thermo Fisher Scientific).

### 2.3. Screening of lymphoblastoid cell lines established from convalescent patients

Peripheral blood from 20 donors who had recovered from COVID-19 was obtained at 30–180 days post-symptom onset under study protocols approved by the NCGM Internal Review Board of Ethics Committee (NCGM-G-003528-02). All donors provided written informed consent for the use of their clinical information and blood components, including serum and peripheral blood mononuclear cells (PBMCs). All blood samples were confirmed to be negative for viral mRNA. PBMCs were isolated from freshly drawn blood and stored at −150 °C until use. One sample was discarded because of hemolysis. B lymphocytes were isolated from PBMCs and infected with Epstein–Barr virus, as previously described (Traggiai et al., 2004), and suspended in RPMI 1640 medium (Nacalai Tesque, Inc.) supplemented with 10% FBS. Epstein–Barr virus-transformed cells (LCLs) were then seeded in 96-well microplates in the presence of irradiated allogeneic feeder cells and cultured at 37 °C in a humidified atmosphere containing 5% $CO_2$ for 2–3 weeks. Antibodies in the culture supernatants were screened for their specificity to the S-trimer of wild-type virus (ACROBiosystems) by enzyme-linked immunosorbent assay (ELISA) as described below. Then, SARS-CoV-2 neutralizing activity in supernatants containing S-trimer-specific antibodies was determined, as described.

### 2.4. Screening of LCLs by ELISA using S protein

ELISA MaxiSorp plates in 96- or 384-well format (Thermo Fisher) were coated with 0.25 μg/mL S-trimer or 0.25 μg/mL S-protein RBD (ACROBiosystems) in phosphate-buffered saline (−) (PBS) at 4 °C overnight. The plates were blocked with 10 mg/mL BlockAce (K.A.C.) for 2 h at room temperature and then incubated with human antibodies diluted in 10% FBS-RPMI 1640 for 1 h at room temperature. Binding antibodies were detected using horseradish peroxidase-labeled anti-human IgG (MBL) and subsequent TMB substrate (Sigma-Aldrich). Isotype- and subclass-specific secondary antibodies (Millipore) were used to identify the isotype and subclass of the antibodies.

### 2.5. Isolation of S-trimer-specific mAbs

LCLs secreting S-trimer-specific antibodies were screened using microwells (Ogunniyi et al., 2009). Briefly, single cells were sorted into an array of microwells and sealed with a glass slide coated with S-trimer. The antibodies secreted from each cell were detected by staining the glass slides with a fluorescently-labeled secondary antibody. Single cells were picked up from the positive wells by manual micromanipulation and transferred into lysis buffer (Cells-to-cDNA Kit; Thermo Fisher Scientific). cDNA was synthesized using SuperScript IV Reverse Transcriptase (Thermo Fisher Scientific) with oligo-dT primers. Variable regions of heavy chains (VHs) and full-length light chains (LCs) were amplified by PCR using KOD-plus DNA polymerase (Toyobo) with primers specific to the 5′-end of each translation initiation site and the 3′-end of the constant region for VHs or the termination sites for LCs. Secondary PCR was performed using primers containing a cloning site for the pcDNA3.1 (+) expression vector (Thermo Fisher Scientific). VHs and LCs of REG10933 and REG10987 were artificially synthesized based on sequence information (WO2021/04586 A1). To generate full-length heavy chains (HCs), the expression vector for VHs was modified to contain the HC constant region of human IgG1. The PCR products were ligated with the expression vector, followed by transformation into *Escherichia coli* DH5α cells. After plasmid isolation, HCs and LCs were sequenced and the complementarity-determining regions were analyzed using the IMGT V-Quest webserver (www.omgt.org; International ImMunoGeneTics Information System). Recombinant antibodies were expressed in ExpiCHO cells (Thermo Fisher Scientific) transiently co-transfected with the HC and LC expression vectors. Antibody purification was performed by affinity chromatography using a prepacked HiTrap rProtein A Fast Flow column (Cytiva).

### 2.6. Surface plasmon resonance (SPR)

SPR measurements were performed using a Biacore T200 system (Cytiva). As the running and dilution buffers, a solution composed of 0.01 M HEPES, 0.15 M NaCl, 3 mM EDTA, and 0.05% surfactant P20 (pH 7.4) (HBS-EP+) was used. All measurements were performed at 25 °C. An anti-IgG (Fc) antibody (Human Antibody Capture Kit; Cytiva) was immobilized on a CM5 sensor chip (Cytiva). mAbs at 0.25 μg/mL were injected over the sensor chip for 300 s at 10 μL/min, and then various concentrations of S-trimer (27 nM–0.33 nM) or RBDs (9 nM–0.11 nM) were injected for 180 s at 30 μL/min. Dissociation was for 1,200 s (S-trimer) or 600 s (RBDs) at a flow rate of 30 μL/min. The kinetic parameters were calculated from the obtained sensorgrams using a 1:1 binding model (Biacore T200 evaluation software 1.0; Cytiva).

For the competition assay, the running and dilution buffers were 50 μM EDTA in 0.01 M HEPES, 0.15 M NaCl, and 0.05% surfactant P20 (pH 7.4) (HBS-P+). Five nM His-tagged RBD of SARS-CoV-2 (ACROBiosystems) was loaded for 60 s at 10 μL/min onto a nitrilotriacetic acid sensor chip (Cytiva) activated with $Ni^{2+}$. Then, a saturating concentration of mAbs was injected for 600 s at 30 μL/min followed by injection of competing mAbs at the same concentration for 180 s at 30 μL/min. The mAb inhibition rate was calculated as the percentage of the binding response obtained from the control antibody.

### 2.7. Preparation of escape mutants and neutralization assay

Escape mutants were obtained as previously described (Baum et al., 2020; Copin et al., 2021). The Delta variant was mixed with REGN-COV diluents (0.016–10 μg/mL) for 1 h at 37 °C and added to VeroE6-TMPRSS2 cells at a multiplicity of infection (MOI) of 1. After 3 days, the supernatant was collected from the wells with the highest mAb concentration that were positive for a complete cytopathic effect. For the subsequent rounds of selection, 10 μL of supernatant containing the virus was passaged by the same procedure until the virus stock could induce a complete cytopathic effect even in the presence of 10 μg/mL REGN-COV. The neutralizing activity of EV053273 and EV053286 on the escape mutants was examined at an MOI of 0.01. Viral RNA was extracted using a QIAamp Viral RNA Mini Kit (Qiagen). Libraries were made using an NEBNext ARTIC SARS-CoV-2 Library Prep Kit for Illumina (E7640; New England BioLabs) and sequenced with the MiSeq system (Illumina). Genomic variants of the RBD were detected by Strand NGS software (Strand Life Sciences).

### 2.8. Antiviral effects of mAbs in mice

Two sets of *in vivo* experiments were performed by intranasally inoculating mice with the QHmusX virus ($2.3 \times 10^3$ TCID50/mouse) (Iwata-Yoshikawa et al., 2022). In the first experiment, 2.5–30 mg/kg mAbs of EV053273, EV053286, cocktail (EV053273+EV053286), and REGN-COV (REG10933+REG10987) in 125 μL PBS were administered intraperitoneally at 1 h after infection with QHmusX. In the second experiment, the mAbs were administered at 1 or 6 h after infection. Control mice were injected with PBS. Body weight was measured daily ($n = 4$–8 per group), and the animals were sacrificed after 3 days to analyze viral replication in lung tissue ($n = 4$ per group). Lung tissue samples from mice were collected at 3 days post-infection and stored at −80 °C. Tissue homogenates (10% w/v) were prepared in Dulbecco's Modified Eagle medium (DMEM) containing 2% FBS, 50 IU/mL penicillin G, and 50 μg/mL streptomycin, and samples were inoculated onto VeroE6/TMPRSS2 cell cultures, which were then examined for cytopathic effects (CPEs) for 5 days. Viral infectivity titers were determined in VeroE6/TMPRSS2 cell cultures using the microtitration assay. Viral infectivity titers were expressed as TCID50/ml and were calculated according to the Behrens–Kärber method.

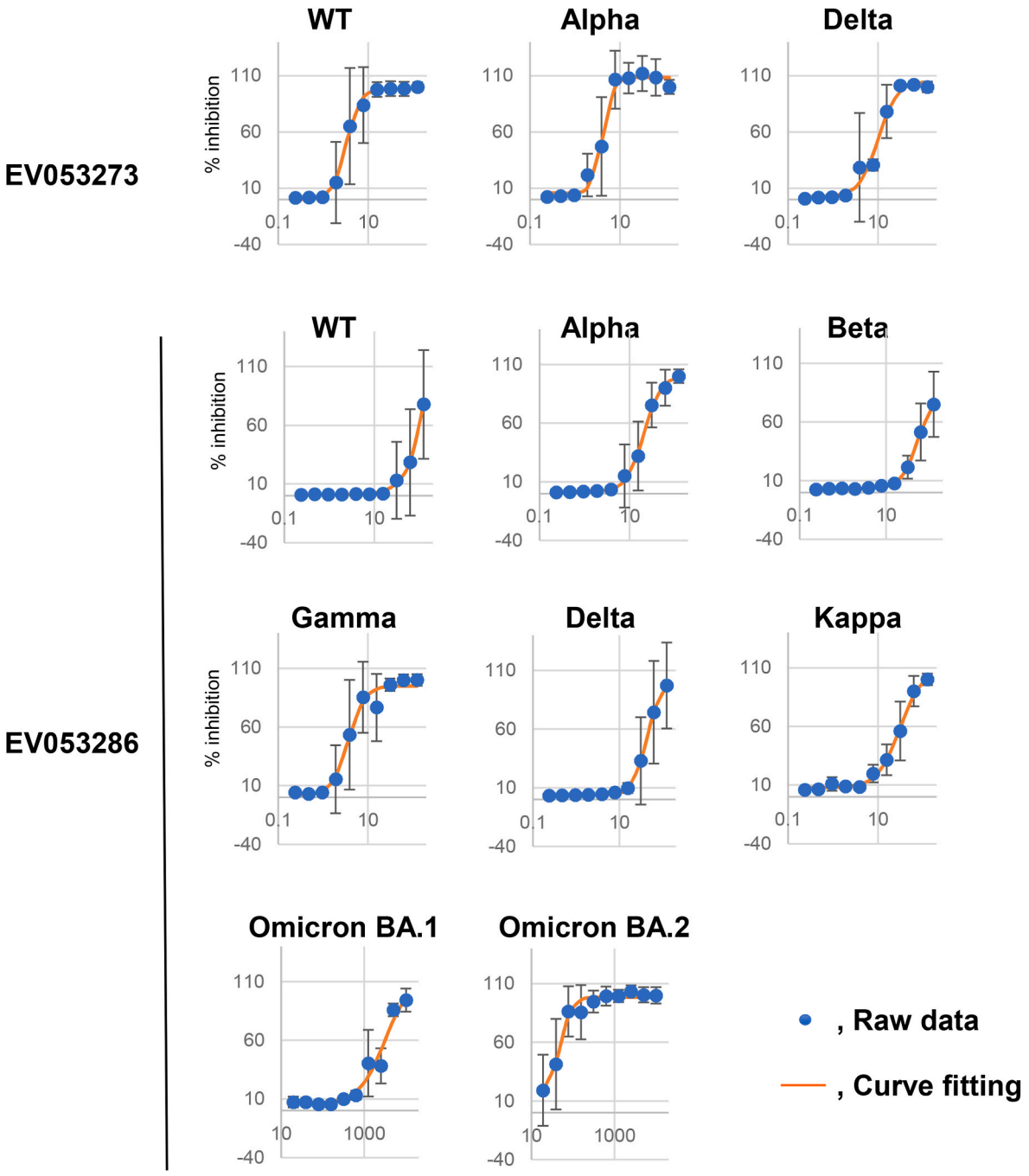


**Fig. 1.** Neutralizing activity against SARS-CoV-2 variants. Dose response curves of neutralization by EV053273 (upper panels) and EV053286 (lower panels) are depicted. mAbs were serially diluted (125–0.24 ng/mL, or 10000-19 ng/mL) and used to infect VeroE6/TMPRSS2 cells. The MOI was 0.01. Data are represented as means ± standard deviation.

### *2.9. Statistical analysis*

Animal experiment data are expressed as the mean and standard error of the mean. Statistical analyses were performed using Prism 9 software (GraphPad Software). Intergroup comparisons were performed using nonparametric analysis. A P value $< 0.05$ was considered statistically significant.

## 3. Results

### *3.1. Identification of EV053273 and EV053286*

By ELISA screening using S-trimer as an antigen, we first selected a total of 150 culture supernatants of LCLs, which were derived from 19 convalescent patients. After serial neutralization assays with the culture supernatants of cells infected with Wuhan wild-type SARS-CoV-2, a total of 30 S-targeting antibodies were cloned and expressed (Supplementary Fig. 1). Of these 30 antibodies, 10 were purified as IgG with neutralizing activity after additional screening with the Alpha, Beta, Gamma, Delta, and Kappa variants (Supplementary Fig. 2).

**Table 1**
IC50 values of mAbs against SARS-CoV-2 variants.

| Antibody | WT | Alpha | Beta | Gamma | Kappa | Delta | Omicron | |
|---|---|---|---|---|---|---|---|---|
| | | | | | | | BA.1 | BA.2 |
| EV053273 | 3.1[a] | 4.0 | – | – | – | 10.3 | – | – |
| EV053286 | 84.5 | 20.8 | 60.3 | 3.7 | 26.3 | 41.6 | 2971.5 | 44.5 |

WT, wild-type.
[a] ng/mL.

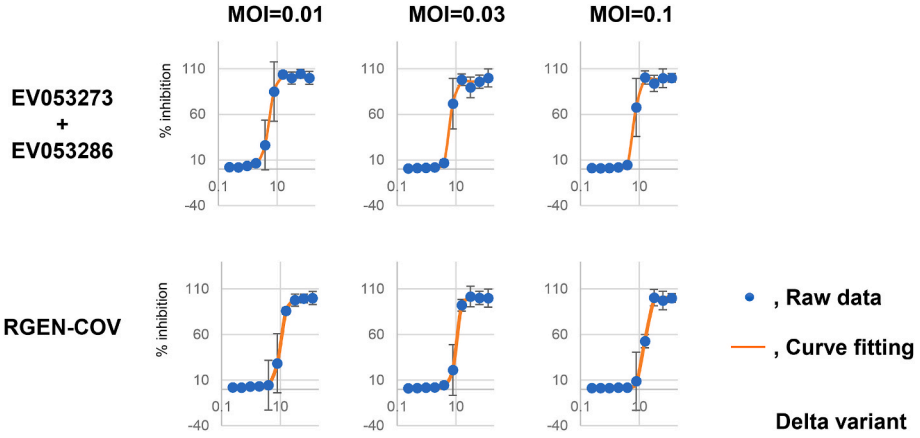


**Fig. 2.** Effects of the combined use of EV053273 and EV053286. The antiviral effects of EV053273 combined with EV053286 (upper panels) and REGN-COV (lower panels) were examined at three different MOIs (0.01, 0.03, and 0.1). The mAbs were serially diluted (125–0.24 ng/mL) and used to infect VeroE6/TMPRSS2 cells. Data are represented as means ± standard deviation.

**Table 2**
IC50 values of mAb cocktails against the Delta variant of SARS-CoV-2.

| mAb | MOI | | |
|---|---|---|---|
| | 0.1 | 0.03 | 0.01 |
| EV053273+EV053286 | 6.4[a] | 6.2 | 5.2 |
| REG10933+REG10987 | 15 | 10.3 | 10.1 |

[a] ng/mL.

Among these, we selected EV053273 and EV053286 for further analysis. EV053273 had the most potent neutralizing activity and could efficiently block infection of wild-type virus and two variants (Alpha and Delta). Its IC50 values were excellent, ranging from 3.1 to 10.3 ng/mL (Fig. 1 and Table 1). In contrast, EV053286 had IC50 values ranging from 3.7 to 84.5 ng/mL depending on the variant, but it could neutralize all viruses analyzed (wild-type, Alpha, Beta, Gamma, Delta, and Kappa) (Fig. 1 and Table 1). Moreover, EV053286 had antiviral activity against the Omicron variants BA.1 and BA.2 with IC50 of 2,971.5 and 44.5 ng/mL, respectively. We next examined the antiviral effects of the combined use of EV053273 and EV053286 on the Delta variant. As shown in Fig. 2 and Table 2, this mAb cocktail had potent neutralizing activity with IC50 values of 5.2–6.4 ng/mL, which was comparable to that of REGN-COV (10.1–15.0 ng/mL). The binding kinetics of these mAbs assessed by an SPR assay revealed that the measured equilibrium constant ($K_D$) of EV053273 and EV053286 with SARS-CoV-2 RBD was $2.66 \times 10^{-10}$ mol/L and $3.84 \times 10^{-10}$ mol/L, respectively.

### 3.2. Antiviral effects of EV053273 and EV053286 on REGN-COV escape mutants

To examine whether the EV053273 and EV053286 cocktail could compensate for the viral escapability of REGN-COV, we obtained mutant viruses by propagating the Delta variant in the presence of 10 μg/mL REGN-COV (Fig. 3A). In the first trial, escape mutants were obtained at passage 13 (escape mutant [EM]-1). In the second trial, EM-2 was obtained at passage 16. The infectivity of EM-1 was blocked by 31.25–125 ng/mL EV053286, but not by EV053273 (Fig. 3B). In contrast, EM-2 was blocked by both EV053273 and EV053286 at a concentration of 31.25 ng/mL (Fig. 3B). By next-generation sequencing analysis, we detected three RDB variants (V445F, F486S, and Y489H). V445F was observed in both escape mutants. F486S was detected in EM-1, whereas Y489H was present in EM-2. It is of note that V445F and F486S were reported in viruses that were derived from patients who were treated with a high dose of REGN-COV and in mice that were administered REG10933 (Copin et al., 2021). In contrast, Y489H was reported as a mutation possibly related to the viral escapability of S2E12, a mAb that has been proposed to have antiviral activity on a broad range of viruses (Starr et al., 2021a).

### 3.3. Antiviral effects of EV053273 and EV053286 in vivo

To validate the effects of the obtained mAbs *in vivo,* we evaluated their antiviral activity by using a mouse model. For this, the QHmusX strain, a mouse-passage isolate from an Alpha variant that induces lethality in aged mice within several days, was used (Iwata-Yoshikawa et al., 2022). In the first experiment, 2.5–30 mg/kg EV053273 or 10 mg/kg REGN-COV was injected intraperitoneally into 7 or 8 mice at 1 h after nasal viral inoculation (Fig. 4A and B). When PBS was injected as a control, all 8 mice displayed severe loss of body weight and died at 6 days post viral infection. In contrast, injections of EV053273 or REGN-COV ameliorated the body weight loss, and all mice, except for one mouse in a group injected with EV053273, survived. The antiviral effects of 10 and 30 mg/kg EV053273 were remarkable as it completely protected against body weight loss in the first few days after viral inoculation. In the second experiment, the antiviral effects of 10 mg/kg EV053273 or 10 or 30 mg/kg EV053286 were examined (n = 6). In the control group, severe body weight loss was observed on day 5 after viral infection, and 3 of 6 mice died (Fig. 4C and D). In contrast, all doses of EV053286 protected against body weight loss and all mice survived. In

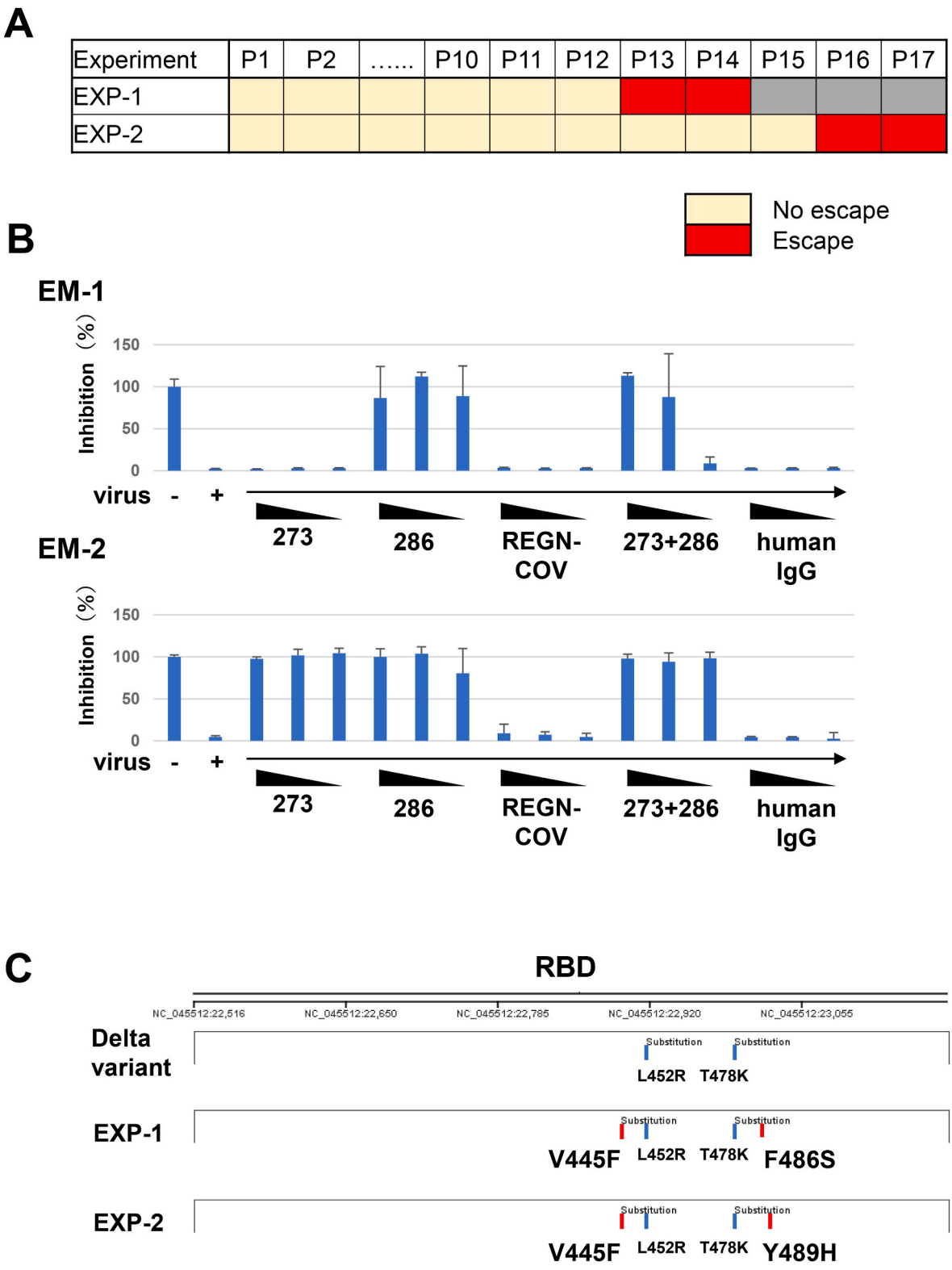


**Fig. 3.** Antiviral effects of EV053273 and EV053286 on REGN-COV escape mutants. (A) Preparation of REGN-COV escape mutants. According to the reported procedures (Baum et al., 2020; Copin et al., 2021), the Delta variant was initially propagated in 16 ng/mL REGN-COV. Then, it was passaged in gradually increasing concentrations of REGN-COV up to a final concentration of 10 μg/mL. In experiment 1 (EXP-1), the escape mutant was obtained at passage 13 (EM-1, red), and in EXP-2, the escape mutant was obtained at passage 16 (EM-2, red). (B) Neutralizing activity of EV053273 and EV053286 against the escape mutants at an MOI of 0.01. EM-1 or EM-2 was reacted with serially diluted EV053273 (273), EV053286 (286), and their cocktail (273 + 286), and then used to infect VeroE6/TMPRSS2 cells. As a negative control, human IgG, a mAb to CMV, was used. Data are represented as means ± standard deviation. (C) Variant analysis of the sequences of the escape mutants. Of note, L452R and T478K were detected as mutated residues of the Delta variant. (For interpretation of the references to colour in this figure legend, the reader is referred to the Web version of this article.)

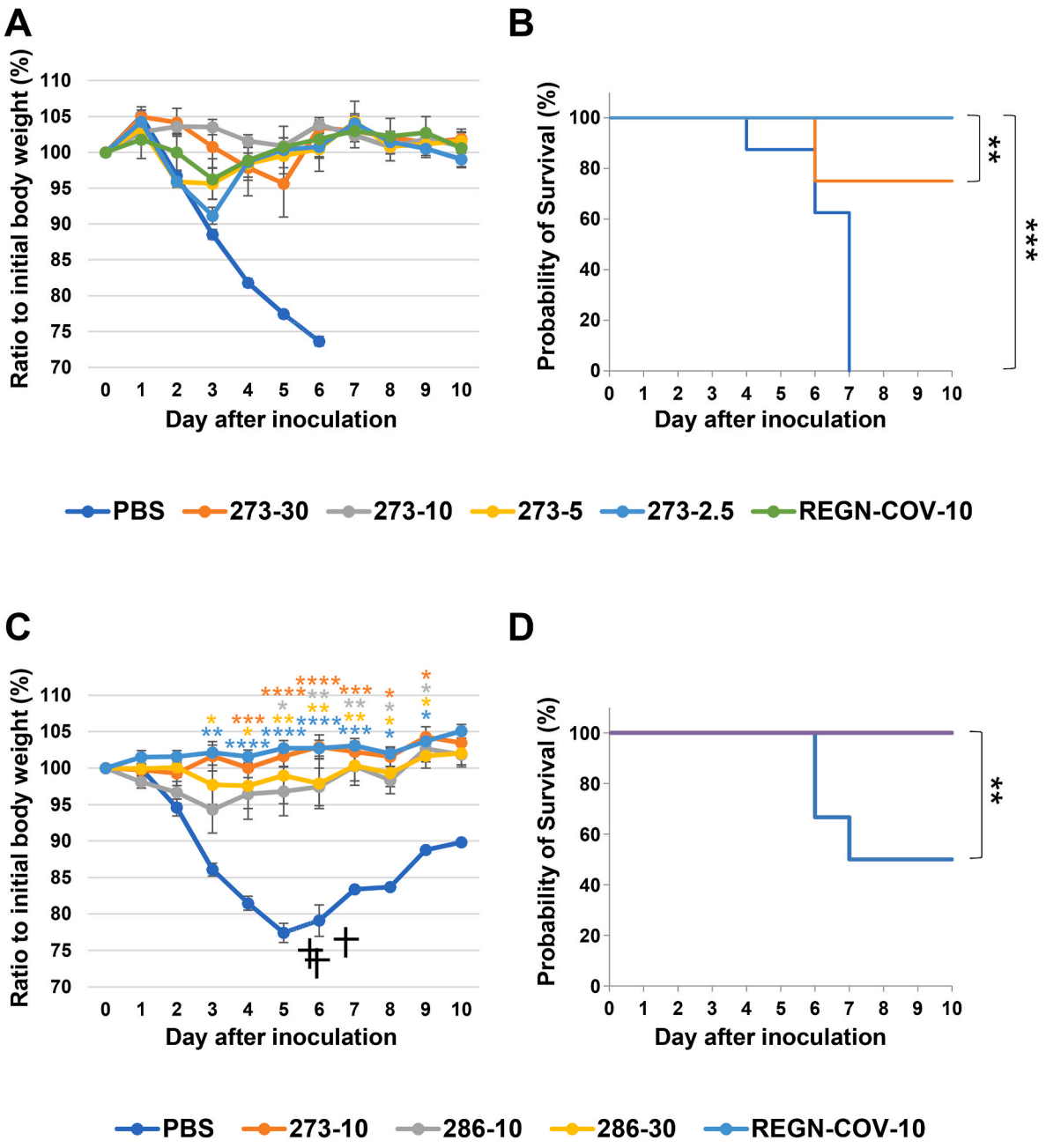


**Fig. 4.** Antiviral effects of EV053273 and EV053286 *in vivo*. The mice were inoculated intranasally with $2.3 \times 10^3$ TCID50 of QHmusX, and then intraperitoneally administered with mAbs at 1 h after infection. (A) Changes of body weight and (B) survival curves of mice in the first experiment. The mice were injected with 2.5, 5, 10, or 30 mg/kg EV053273 (273-2.5, −5, −10, and −30) or 10 mg/kg REGN-COV (REGN-COV-10). 8 mice were used for 273–2.5, 5 and 30 and PBS (control). 7 mice were used for 273 - 10 and REGN-COV - 10. Injection of PBS induced remarkable body weight loss, and the injected mice died on day 6. One of 7 mice injected with 30 mg/kg EV053273 died on day 5. (C) Body weight changes and (D) survival curves of mice in the second experiment. The effects of 10 or 30 mg/kg EV053286 (286-10 or −30) were compared with those of 10 mg/kg EV053273 (273-10) or 10 mg/kg REGN-COV (REGN-COV-10). For each dose of mAb, 6 mice were used. Asterisks indicate statistically significant differences compared with the PBS-injected mice, which were estimated by Dunnett's multiple comparisons test for body weight or by a log-rank (Mantel–Cox) test for survival. *P < 0.05, **P < 0.01, ***P < 0.001. Data are represented as means ± standard deviation.

the third experiment, we estimated viral titers in the lung tissue of mice on day 3 after viral challenge. In this experiment, the mAbs were injected at 1 or 6 h after viral inoculation (n = 4). When the mAbs were administered at 1 h after viral inoculation, no apparent body weight loss was observed (Fig. 5A, left panel), and qRT-PCR analysis revealed that 10 mg/kg EV053286 with or without 10 mg/kg EV053273 significantly blocked viral replication (Fig. 5B, left panel). When 10 or 30 mg/kg EV053286 or 10 mg/kg EV053273 was injected at 6 h after viral inoculation, body weight loss was observed on day 2 after viral inoculation, but recovered on day 3 (Fig. 5A, right panel). qRT-PCR analysis revealed that both EV053273 and EV053286 blocked viral replication. These data indicated that the antiviral effect of each mAb was comparable to that of REGN-COV *in vivo* (Fig. 5B, right panel).

## 4. Discussion

Here, we characterized two mAbs targeting the S protein of SARS-CoV-2. The neutralizing activity of EV053273 was especially potent and blocked infection with the Wuhan wild-type virus as well as the Alpha and Delta variants at single digit ng/mL concentrations. In

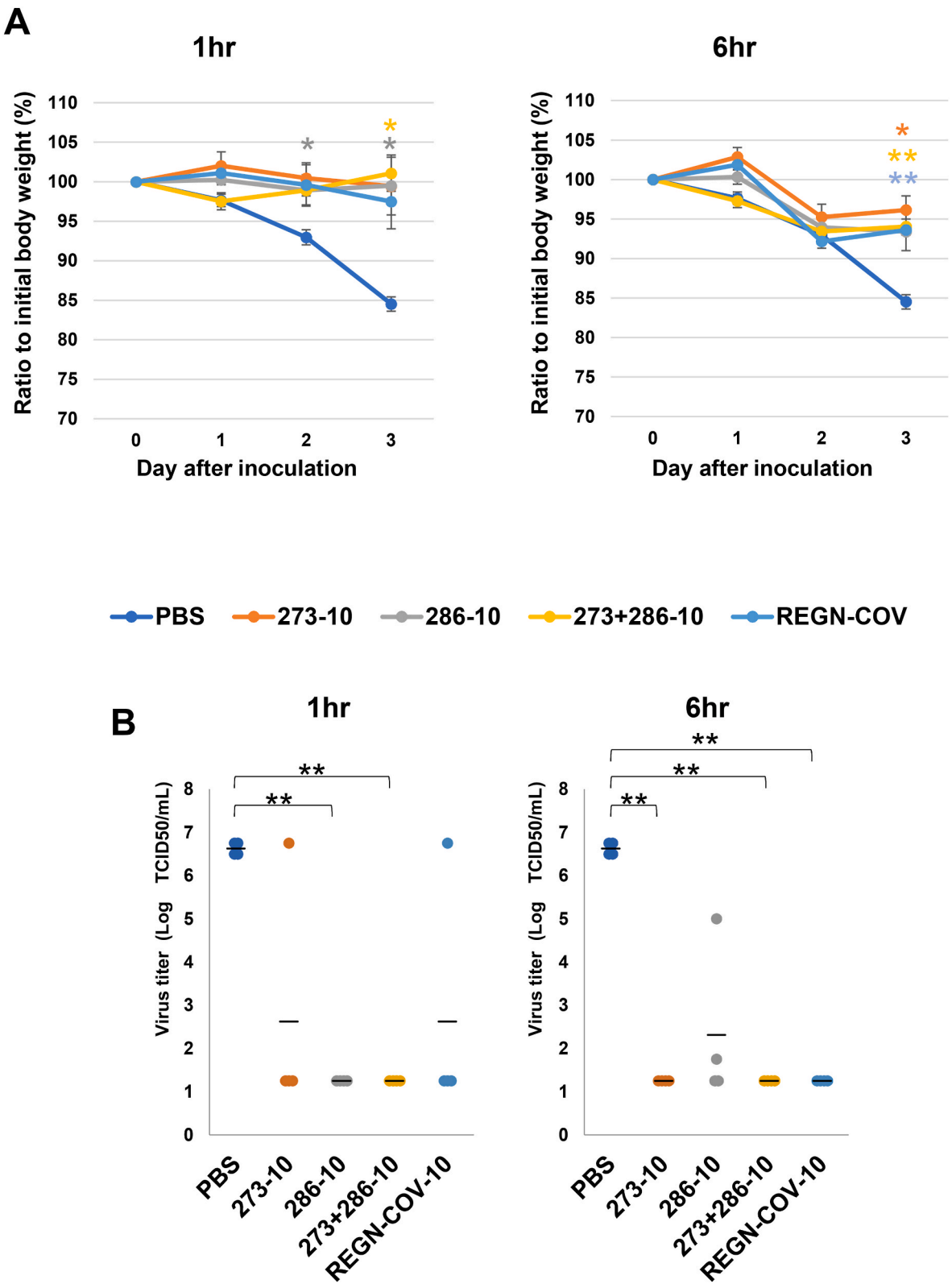


**Fig. 5.** Antiviral effects of EV053273 and EV053286 injected at 1 and 6 h after viral challenge. The mAbs were injected intraperitoneally at 1 (left panels) or 6 h (right panels) after inoculation with $2.3 \times 10^3$ TCID50 of QHmusX. For each dose of mAb, 4 mice were used. (A) Changes of body weight. The mice were injected with 10 mg/kg EV053273 (273-10), EV053286 (286-10), EV053273 plus EV053286 (273 + 286-10), or REGN-COV (REGN-COV-10). Asterisks indicate statistically significant differences, estimated by Dunnett's multiple comparisons test. *$P < 0.05$ and **$P < 0.01$. (B) Viral titers in lung homogenates on day 3. Samples obtained from the experiment shown in (A) were subjected to viral infectivity titers analysis. Asterisks indicate statistically significant differences evaluated by Dunn's multiple comparison test following the Kruskal-Walls test. *$P < 0.05$ and **$P < 0.01$. Data are represented as means ± standard deviation.

**Table 3**
Characterization of the mAbs.

| mAb | Days after onset | Disease severity | Properties of the antibody | | |
|---|---|---|---|---|---|
| | | | *VH* gene (% identity) | HCDR3 (aa) | *VL* gene (% identity) |
| EV053273 | 121 | Mod | IGHV1-2*02 (95.49) | ARDNSWSTVQFCLDY | IGLV2-8*01 (98.26) |
| EV053286 | 74 | Mild | IGHV3-53*01 (97.19) | ARDLPHIAATGRV | IGKV1-33*01 (98.21) |

VH and VL % identity refers to V gene segment identity compared to germline (as per IMGT; http://www.imgt.org). Mod, moderate clinical symptoms.

contrast, the activity of EV053286 varied depending on the virus, but it inhibited a wide range of viruses at double-digit ng/mL concentrations with potent antiviral activity to the Gamma variant (IC50, 3.7 ng/mL) (Table 1). When 2.5–10 mg/kg of each mAb was injected into mice, EV053286 with EV053273 demonstrated comparable antiviral effects (Figs. 4 and 5). Data indicate that differences in the IC50 values of mAbs estimated by *in vitro* experiments are subtle when more than several mg/kg of mAb is applied *in vivo* (Cruz-Teran et al., 2021), also suggesting that it is imperative to stockpile such mAbs with action against a broad spectrum of variants, even though their antiviral effect *in vitro* is not strictly potent.

Independent experiments revealed that EV053273 and EV053286 efficiently blocked the infectivity of mutant viruses that emerged under antiviral pressure by REGN-COV (REG10987 and REG10933). Of note, EV053286 had consistent antiviral activity on the escape mutants that were generated in two independent experiments (Fig. 3). Next-generation sequencing analysis identified the amino acid alterations V445F, F486S, and Y489H in the escape mutants. Notably, V445F and F486S have been detected in patients and mice administered REGN-COV or REG10933 (Copin et al., 2021). In contrast, Y489H was reported in a panel of candidate escape mutants of S2E12, a mAb that has antiviral activity on a broad range of viruses, although it recognizes the receptor-binding motif of the S protein of SARS-CoV-2, by which it attaches directly to ACE2 (Starr et al., 2021a). To understand the mode by which EV053286 has an effect on a broad range of variant viruses, we performed an SPR competition assay on RBD and observed that EV053286 did not compete with REG10987 (Supplementary Fig. 3). These data support the idea that EV053286 can co-operate with REG10987. However, EV053273 competed with both REG10987 and REG10933, implying that fine structural analysis is required for further characterization of EV053286.

EV053273 and EV053286 were isolated from PBMCs that were prepared from convalescent patients on days 121 and 74 after the onset of viral infection, respectively. Nucleotide sequence analysis revealed that EV053273 and EV053286 were derived from *VH1-2* and *VH3-53*, respectively, which are commonly utilized genes for SARS-CoV-2 IgG production (Rapp et al., 2021). Rapp et al. (2021) recently proposed that *VH1-2*-encoded IgG has the characteristics of public antibodies, which are commonly generated among infected patients. Public antibodies have been found in influenza (Wrammert et al., 2011) and human immunodeficiency virus type 1 (Scheid et al., 2009). *VH1-2*-encoded mAbs have heavy-chain complementarity-determining region 3 (CDRH3), which consists of 11–21 amino acids (aa) and commonly bind to the receptor-binding motif. This is the reason why *VH1-2*-encoded mAbs have potent antiviral activity. However, importantly, Y449, E484, F486, and Q493 are known as critical residues for the interaction of *VH1-2*-encoded mAbs with the receptor-binding motif, consistent with the observation that EV053273 had no antiviral activity to the Lambda, Gamma, and Omicron variants. The Lambda and Gamma variants have a mutation at E484, whereas the Omicron variant has a mutation at Q493. In contrast, mAbs encoded by *VH3-53* with a short CDRH3 (11 or 12 aa) has been shown to bind to the "up" form of the RBD, which is the form competent for ACE2 binding (Wu et al., 2020a), whereas approximately 10% of *VH3-53*-derived IgG possesses a longer CDRH3 (>15 aa) (Barnes et al., 2020a) and rotation of Fab by 180° due to a long CDRH3 promotes the molecule to bind to both the "up" and "down" forms of the RBD. EV053286 has a CDRH3 of 13 aa, suggesting that EV053286 binds to the "up" form of the RBD. It is important to obtain further information on the mode of the interaction of EV053286 and the RBD, which will enable us to identify a critical area of the RBD for IgG targeting a broad spectrum of variant viruses.

The frequency of mismatch in the *VHs* of EV053273 and EV053286 was 4.51% and 2.81%, respectively, whereas those of variable light chain (VL) genes were 1.76% and 1.79% (Table 3). The frequency of somatic mutations in cloned mAbs to SARS-CoV-2 is generally low, compared with those from patients with chronic infection (Robbiani et al., 2020). The average frequency of nucleotide mutations in VH is 4.2% in SARS-CoV-2 patients, while those of patients with hepatitis B (Muecksch et al., 2021a; Wang et al., 2020) and human immunodeficiency virus type 1 (Scheid et al., 2009) are high, ranging from 20% to 30%. A recent study proposed that approximately 90% of virus-specific effector cells for SARS-CoV-2 die, whereas 10% persist as long-lived memory cells (Ruterbusch et al., 2020), and *VH* genes are susceptible to somatic hypermutations in memory B cells for at least 6 months after diagnosis with an increase of antiviral activity and a wider range of target viruses (Muecksch et al., 2021a). EV053286 was isolated from PBMCs that were prepared on day 74 after infection, and it is plausible that EV053286-encoding IgG, for example, when isolated 1 year later, would exert more potent antiviral activity on the Omicron variant.

## 5. Conclusion

The mAbs EV053273 and EV053286 were identified from convalescent patients who were infected with Wuhan wild-type SARS-CoV-2. The combined use of EV053273 and EV053286 had comparable antiviral effects with REGN-COV, which is used to treat patients with COVID-19, and could block the infectivity of REGN-COV escape mutants. Especially, EV053286 could neutralize the Omicron variants BA.1 and BA.2. These data suggest that EV053273 and EV053286 represent a novel option as antibody therapy for SARS-CoV-2.

## Author contributions

M.U., N. I.-Y., T. O., N. S.-S., N. N., T. S., A. S., M. O., and Y. T. performed experiments. M. U., A. M., K. S., N. N., M. O., R. M., and Y. I. prepared a manuscript. S. S., S. A., S. K., M. K., and N. O. coordinated patient recruitment. I. Y., M. N., H. A., Y. I. Y., J. S., K. S., and K. Y. isolated virus variants.

## Declaration of competing interest

The authors declare the following financial interests/personal relationships which may be considered as potential competing interests: Sho Saito, Satoshi Kutsuna and Yukihito Ishizaka have received research grants from EVEC, Inc. EVEC, Inc., has received research grants from "Northern advancement center for science and technology" and "Foundation for Biomedical Research and Innovation at Kobe". Mikako Ueno, Sho Saito, Satoshi Kutsuna, Moto Kimura, Ryu Miura, and Yukihito Ishizaka are holders of patents describing the EV053273 and EV053286 antibodies reported here.

## Acknowledgments

This study was supported in part by Grants-in-Aid from the National Center for Global Health and Medicine, Japan (E20A2004D01, 20A2010, 20A2007D); the Research Program on Emerging and Re-emerging Infectious Diseases from AMED, Japan, under Grant Number

JP 20fk0108262, 20fk0108411, 20fk0108511; KBIC Research Grants-in-Aid for Collaborative Projects by Kobe City, Japan; and an Infectious Disease Control Medical Care, Prevention-related Development Subsidy from the City of Sapporo and the Northern Advancement Center for Science & Technology of Hokkaido, Japan. We are grateful to Drs. Tohru Akiyama, Kenji Maeda, Kiyoto Tsuchiya, Kazuo Yoshida, Shinichiro Morioka for their help in the current work. We would like to thank Mses. Mari Terada, Kozue Takahashi and Yumiko Shimanishi for their help with patient enrollment.

## Appendix A. Supplementary data

Supplementary data to this article can be found online at https://doi.org/10.1016/j.antiviral.2022.105297.

## References

Barnes, C.O., Jette, C.A., Abernathy, M.E., Dam, K.A., Esswein, S.R., Gristick, H.B., Malyutin, A.G., Sharaf, N.G., Huey-Tubman, K.E., Lee, Y.E., Robbiani, D.F., Nussenzweig, M.C., West Jr., A.P., Bjorkman, P.J., 2020a. SARS-CoV-2 neutralizing antibody structures inform therapeutic strategies. Nature 588, 682–687.

Barnes, C.O., West Jr., A.P., Huey-Tubman, K.E., Hoffmann, M.A.G., Sharaf, N.G., Hoffman, P.R., Koranda, N., Gristick, H.B., Gaebler, C., Muecksch, F., Lorenzi, J.C.C., Finkin, S., Hagglof, T., Hurley, A., Millard, K.G., Weisblum, Y., Schmidt, F., Hatziioannou, T., Bieniasz, P.D., Caskey, M., Robbiani, D.F., Nussenzweig, M.C., Bjorkman, P.J., 2020b. Structures of human antibodies bound to SARS-CoV-2 spike reveal common epitopes and recurrent features of antibodies. Cell 182, 828-842.e16.

Baum, A., Fulton, B.O., Wloga, E., Copin, R., Pascal, K.E., Russo, V., Giordano, S., Lanza, K., Negron, N., Ni, M., Wei, Y., Atwal, G.S., Murphy, A.J., Stahl, N., Yancopoulos, G.D., Kyratsous, C.A., 2020. Antibody cocktail to SARS-CoV-2 spike protein prevents rapid mutational escape seen with individual antibodies. Science 369, 1014–1018.

Brouwer, P.J.M., Caniels, T.G., van der Straten, K., Snitselaar, J.L., Aldon, Y., Bangaru, S., Torres, J.L., Okba, N.M.A., Claireaux, M., Kerster, G., Bentlage, A.E.H., van Haaren, M.M., Guerra, D., Burger, J.A., Schermer, E.E., Verheul, K.D., van der Velde, N., van der Kooi, A., van Schooten, J., van Breemen, M.J., Bijl, T.P.L., Sliepen, K., Aartse, A., Derking, R., Bontjer, I., Kootstra, N.A., Wiersinga, W.J., Vidarsson, G., Haagmans, B.L., Ward, A.B., de Bree, G.J., Sanders, R.W., van Gils, M. J., 2020. Potent neutralizing antibodies from COVID-19 patients define multiple targets of vulnerability. Science 369, 643–650.

Cao, Y., Su, B., Guo, X., Sun, W., Deng, Y., Bao, L., Zhu, Q., Zhang, X., Zheng, Y., Geng, C., Chai, X., He, R., Li, X., Lv, Q., Zhu, H., Deng, W., Xu, Y., Wang, Y., Qiao, L., Tan, Y., Song, L., Wang, G., Du, X., Gao, N., Liu, J., Xiao, J., Su, X.D., Du, Z., Feng, Y., Qin, C., Qin, C., Jin, R., Xie, X.S., 2020. Potent neutralizing antibodies against SARS-CoV-2 identified by high-throughput single-cell sequencing of convalescent patients' B cells. Cell 182, 73–84 e16.

Chen, J., Wang, R., Wang, M., Wei, G.W., 2020. Mutations strengthened SARS-CoV-2 infectivity. J. Mol. Biol. 432, 5212–5226.

Chen, P., Nirula, A., Heller, B., Gottlieb, R.L., Boscia, J., Morris, J., Huhn, G., Cardona, J., Mocherla, B., Stosor, V., Shawa, I., Adams, A.C., Van Naarden, J., Custer, K.L., Shen, L., Durante, M., Oakley, G., Schade, A.E., Sabo, J., Patel, D.R., Klekotka, P., Skovronsky, D.M., Investigators, BLAZE, 2021. SARS-CoV-2 neutralizing antibody LY-CoV555 in outpatients with covid-19. N. Engl. J. Med. 384, 229–237.

Chi, X., Yan, R., Zhang, J., Zhang, G., Zhang, Y., Hao, M., Zhang, Z., Fan, P., Dong, Y., Yang, Y., Chen, Z., Guo, Y., Zhang, J., Li, Y., Song, X., Chen, Y., Xia, L., Fu, L., Hou, L., Xu, J., Yu, C., Li, J., Zhou, Q., Chen, W., 2020. A neutralizing human antibody binds to the N-terminal domain of the Spike protein of SARS-CoV-2. Science 369, 650–655.

Copin, R., Baum, A., Wloga, E., Pascal, K.E., Giordano, S., Fulton, B.O., Zhou, A., Negron, N., Lanza, K., Chan, N., Coppola, A., Chiu, J., Ni, M., Wei, Y., Atwal, G.S., Hernandez, A.R., Saotome, K., Zhou, Y., Franklin, M.C., Hooper, A.T., McCarthy, S., Hamon, S., Hamilton, J.D., Staples, H.M., Alfson, K., Carrion Jr., R., Ali, S., Norton, T., Somersan-Karakaya, S., Sivapalasingam, S., Herman, G.A., Weinreich, D. M., Lipsich, L., Stahl, N., Murphy, A.J., Yancopoulos, G.D., Kyratsous, C.A., 2021. The monoclonal antibody combination REGEN-COV protects against SARS-CoV-2 mutational escape in preclinical and human studies. Cell 184, 3949–3961.e11.

Cruz-Teran, C., Tiruthani, K., McSweeney, M., Ma, A., Pickles, R., Lai, S.K., 2021. Challenges and opportunities for antiviral monoclonal antibodies as COVID-19 therapy. Adv. Drug Deliv. Rev. 169, 100–117.

Fischer, W., Eron, J.J., Holman, W., Cohen, M.S., Fang, L., Szewczyk, L.J., Sheahan, T.P., Baric, R., Mollan, K.R., Wolfe, C.R., Duke, E.R., Azizad, M.M., Borroto-Esoda, K., Wohl, D.A., Loftis, A.J., Alabanza, P., Lipansky, F., Painter, W.P., 2022. A phase 2a clinical trial of molnupiravir in patients with COVID-19 shows accelerated SARS-CoV-2 RNA clearance and elimination of infectious virus. Sci. Transl. Med. 14, eabl7430.

Gaebler, C., Wang, Z., Lorenzi, J.C.C., Muecksch, F., Finkin, S., Tokuyama, M., Cho, A., Jankovic, M., Schaefer-Babajew, D., Oliveira, T.Y., Cipolla, M., Viant, C., Barnes, C. O., Bram, Y., Breton, G., Hagglof, T., Mendoza, P., Hurley, A., Turroja, M., Gordon, K., Millard, K.G., Ramos, V., Schmidt, F., Weisblum, Y., Jha, D., Tankelevich, M., Martinez-Delgado, G., Yee, J., Patel, R., Dizon, J., Unson-O'Brien, C., Shimeliovich, I., Robbiani, D.F., Zhao, Z., Gazumyan, A., Schwartz, R.E., Hatziioannou, T., Bjorkman, P.J., Mehandru, S., Bieniasz, P.D., Caskey, M., Nussenzweig, M.C., 2021. Evolution of antibody immunity to SARS-CoV-2. Nature 591, 639–644.

Gottlieb, R.L., Nirula, A., Chen, P., Boscia, J., Heller, B., Morris, J., Huhn, G., Cardona, J., Mocherla, B., Stosor, V., Shawa, I., Kumar, P., Adams, A.C., Van Naarden, J., Custer, K.L., Durante, M., Oakley, G., Schade, A.E., Holzer, T.R., Ebert, P.J., Higgs, R. E., Kallewaard, N.L., Sabo, J., Patel, D.R., Klekotka, P., Shen, L., Skovronsky, D.M., 2021. Effect of bamlanivimab as monotherapy or in combination with etesevimab on viral load in patients with mild to moderate COVID-19: a randomized clinical trial. JAMA 325, 632–644.

Hansen, J., Baum, A., Pascal, K.E., Russo, V., Giordano, S., Wloga, E., Fulton, B.O., Yan, Y., Koon, K., Patel, K., Chung, K.M., Hermann, A., Ullman, E., Cruz, J., Rafique, A., Huang, T., Fairhurst, J., Libertiny, C., Malbec, M., Lee, W.Y., Welsh, R., Farr, G., Pennington, S., Deshpande, D., Cheng, J., Watty, A., Bouffard, P., Babb, R., Levenkova, N., Chen, C., Zhang, B., Romero Hernandez, A., Saotome, K., Zhou, Y., Franklin, M., Sivapalasingam, S., Lye, D.C., Weston, S., Logue, J., Haupt, R., Frieman, M., Chen, G., Olson, W., Murphy, A.J., Stahl, N., Yancopoulos, G.D., Kyratsous, C.A., 2020. Studies in humanized mice and convalescent humans yield a SARS-CoV-2 antibody cocktail. Science 369, 1010–1014.

Iwata-Yoshikawa, N., Shiwa, N., Sekizuka, T., Sano, K., Ainai, A., Hemmi, T., Kataoka, M., Kuroda, M., Hasegawa, H., Suzuki, T., Nagata, N., 2022. A lethal mouse model for evaluating vaccine-associated enhanced respiratory disease during SARS-CoV-2 infection. Sci. Adv. 8, eabh3827.

Ju, B., Zhang, Q., Ge, J., Wang, R., Sun, J., Ge, X., Yu, J., Shan, S., Zhou, B., Song, S., Tang, X., Yu, J., Lan, J., Yuan, J., Wang, H., Zhao, J., Zhang, S., Wang, Y., Shi, X., Liu, L., Zhao, J., Wang, X., Zhang, Z., Zhang, L., 2020. Human neutralizing antibodies elicited by SARS-CoV-2 infection. Nature 584, 115–119.

Kutsuna, S., 2020. Coronavirus disease 2019 (COVID-19): research progress and clinical practice. Global Health. Med. 2, 78–88.

Kutsuna, S., Asai, Y., Matsunaga, A., 2020. Loss of anti-SARS-CoV-2 antibodies in mild covid-19. N. Engl. J. Med. 383, 1695–1696.

Moriyama, S., Adachi, Y., Sato, T., Tonouchi, K., Sun, L., Fukushi, S., Yamada, S., Kinoshita, H., Nojima, K., Kanno, T., Tobiume, M., Ishijima, K., Kuroda, Y., Park, E. S., Onodera, T., Matsumura, T., Takano, T., Terahara, K., Isogawa, M., Nishiyama, A., Kawana-Tachikawa, A., Shinkai, M., Tachikawa, N., Nakamura, S., Okai, T., Okuma, K., Matano, T., Fujimoto, T., Maeda, K., Ohnishi, M., Wakita, T., Suzuki, T., Takahashi, Y., 2021. Temporal maturation of neutralizing antibodies in COVID-19 convalescent individuals improves potency and breadth to circulating SARS-CoV-2 variants. Immunity 54, 1841–1852.e4.

Muecksch, F., Weisblum, Y., Barnes, C.O., Schmidt, F., Schaefer-Babajew, D., Wang, Z., Lorenzi, J.C.C., Flyak, A.I., DeLaitsch, A.T., Huey-Tubman, K.E., Hou, S., Schiffer, C. A., Gaebler, C., Da Silva, J., Poston, D., Finkin, S., Cho, A., Cipolla, M., Oliveira, T.Y., Millard, K.G., Ramos, V., Gazumyan, A., Rutkowska, M., Caskey, M., Nussenzweig, M.C., Bjorkman, P.J., Hatziioannou, T., Bieniasz, P.D., 2021a. Affinity maturation of SARS-CoV-2 neutralizing antibodies confers potency, breadth, and resilience to viral escape mutations. Immunity 54, 1853-1868.e7.

Muecksch, F., Wise, H., Batchelor, B., Squires, M., Semple, E., Richardson, C., McGuire, J., Clearly, S., Furrie, E., Greig, N., Hay, G., Templeton, K., Lorenzi, J.C.C., Hatziioannou, T., Jenks, S., Bieniasz, P.D., 2021b. Longitudinal serological analysis and neutralizing antibody levels in coronavirus disease 2019 convalescent patients. J. Infect. Dis. 223, 389–398.

Ogunniyi, A.O., Story, C.M., Papa, E., Guillen, E., Love, J.C., 2009. Screening individual hybridomas by microengraving to discover monoclonal antibodies. Nat. Protoc. 4, 767–782.

Rapp, M., Guo, Y., Reddem, E.R., Yu, J., Liu, L., Wang, P., Cerutti, G., Katsamba, P., Bimela, J.S., Bahna, F.A., Mannepalli, S.M., Zhang, B., Kwong, P.D., Huang, Y., Ho, D.D., Shapiro, L., Sheng, Z., 2021. Modular basis for potent SARS-CoV-2 neutralization by a prevalent VH1-2-derived antibody class. Cell Rep 35, 108950.

Robbiani, D.F., Gaebler, C., Muecksch, F., Lorenzi, J.C.C., Wang, Z., Cho, A., Agudelo, M., Barnes, C.O., Gazumyan, A., Finkin, S., Hagglof, T., Oliveira, T.Y., Viant, C., Hurley, A., Hoffmann, H.H., Millard, K.G., Kost, R.G., Cipolla, M., Gordon, K., Bianchini, F., Chen, S.T., Ramos, V., Patel, R., Dizon, J., Shimeliovich, I., Mendoza, P., Hartweger, H., Nogueira, L., Pack, M., Horowitz, J., Schmidt, F., Weisblum, Y., Michailidis, E., Ashbrook, A.W., Waltari, E., Pak, J.E., Huey-Tubman, K.E., Koranda, N., Hoffman, P.R., West Jr., A.P., Rice, C.M., Hatziioannou, T., Bjorkman, P.J., Bieniasz, P.D., Caskey, M., Nussenzweig, M.C., 2020. Convergent antibody responses to SARS-CoV-2 in convalescent individuals. Nature 584, 437–442.

Rogers, T.F., Zhao, F., Huang, D., Beutler, N., Burns, A., He, W.T., Limbo, O., Smith, C., Song, G., Woehl, J., Yang, L., Abbott, R.K., Callaghan, S., Garcia, E., Hurtado, J., Parren, M., Peng, L., Ramirez, S., Ricketts, J., Ricciardi, M.J., Rawlings, S.A., Wu, N. C., Yuan, M., Smith, D.M., Nemazee, D., Teijaro, J.R., Voss, J.E., Wilson, I.A., Andrabi, R., Briney, B., Landais, E., Sok, D., Jardine, J.G., Burton, D.R., 2020. Isolation of potent SARS-CoV-2 neutralizing antibodies and protection from disease in a small animal model. Science 369, 956–963.

Ruterbusch, M., Pruner, K.B., Shehata, L., Pepper, M., 2020. In vivo CD4(+) T cell differentiation and function: revisiting the Th1/Th2 paradigm. Annu. Rev. Immunol. 38, 705–725.

Sakharkar, M., Rappazzo, C.G., Wieland-Alter, W.F., Hsieh, C.L., Wrapp, D., Esterman, E. S., Kaku, C.I., Wec, A.Z., Geoghegan, J.C., McLellan, J.S., Connor, R.I., Wright, P.F., Walker, L.M., 2021. Prolonged evolution of the human B cell response to SARS-CoV-2 infection. Sci. Immunol. 6, eabg6916.

Scheid, J.F., Mouquet, H., Feldhahn, N., Seaman, M.S., Velinzon, K., Pietzsch, J., Ott, R. G., Anthony, R.M., Zebroski, H., Hurley, A., Phogat, A., Chakrabarti, B., Li, Y., Connors, M., Pereyra, F., Walker, B.D., Wardemann, H., Ho, D., Wyatt, R.T., Mascola, J.R., Ravetch, J.V., Nussenzweig, M.C., 2009. Broad diversity of

neutralizing antibodies isolated from memory B cells in HIV-infected individuals. Nature 458, 636–640.
Seydoux, E., Homad, L.J., MacCamy, A.J., Parks, K.R., Hurlburt, N.K., Jennewein, M.F., Akins, N.R., Stuart, A.B., Wan, Y.H., Feng, J., Whaley, R.E., Singh, S., Boeckh, M., Cohen, K.W., McElrath, M.J., Englund, J.A., Chu, H.Y., Pancera, M., McGuire, A.T., Stamatatos, L., 2020. Analysis of a SARS-CoV-2-infected individual reveals development of potent neutralizing antibodies with limited somatic mutation. Immunity 53, 98–105.e5.
Shi, R., Shan, C., Duan, X., Chen, Z., Liu, P., Song, J., Song, T., Bi, X., Han, C., Wu, L., Gao, G., Hu, X., Zhang, Y., Tong, Z., Huang, W., Liu, W.J., Wu, G., Zhang, B., Wang, L., Qi, J., Feng, H., Wang, F.S., Wang, Q., Gao, G.F., Yuan, Z., Yan, J., 2020. A human neutralizing antibody targets the receptor-binding site of SARS-CoV-2. Nature 584, 120–124.
Sokal, A., Chappert, P., Barba-Spaeth, G., Roeser, A., Fourati, S., Azzaoui, I., Vandenberghe, A., Fernandez, I., Meola, A., Bouvier-Alias, M., Crickx, E., Beldi-Ferchiou, A., Hue, S., Languille, L., Michel, M., Baloul, S., Noizat-Pirenne, F., Luka, M., Megret, J., Menager, M., Pawlotsky, J.M., Fillatreau, S., Rey, F.A., Weill, J. C., Reynaud, C.A., Mahevas, M., 2021. Maturation and persistence of the anti-SARS-CoV-2 memory B cell response. Cell 184, 1201–1213.e14.
Starr, T.N., Czudnochowski, N., Liu, Z., Zatta, F., Park, Y.J., Addetia, A., Pinto, D., Beltramello, M., Hernandez, P., Greaney, A.J., Marzi, R., Glass, W.G., Zhang, I., Dingens, A.S., Bowen, J.E., Tortorici, M.A., Walls, A.C., Wojcechowskyj, J.A., De Marco, A., Rosen, L.E., Zhou, J., Montiel-Ruiz, M., Kaiser, H., Dillen, J.R., Tucker, H., Bassi, J., Silacci-Fregni, C., Housley, M.P., di Iulio, J., Lombardo, G., Agostini, M., Sprugasci, N., Culap, K., Jaconi, S., Meury, M., Dellota Jr., E., Abdelnabi, R., Foo, S. C., Cameroni, E., Stumpf, S., Croll, T.I., Nix, J.C., Havenar-Daughton, C., Piccoli, L., Benigni, F., Neyts, J., Telenti, A., Lempp, F.A., Pizzuto, M.S., Chodera, J.D., Hebner, C.M., Virgin, H.W., Whelan, S.P.J., Veesler, D., Corti, D., Bloom, J.D., Snell, G., 2021a. SARS-CoV-2 RBD antibodies that maximize breadth and resistance to escape. Nature 597, 97–102.
Starr, T.N., Greaney, A.J., Addetia, A., Hannon, W.W., Choudhary, M.C., Dingens, A.S., Li, J.Z., Bloom, J.D., 2021b. Prospective mapping of viral mutations that escape antibodies used to treat COVID-19. Science 371, 850–854.
Traggiai, E., Becker, S., Subbarao, K., Kolesnikova, L., Uematsu, Y., Gismondo, M.R., Murphy, B.R., Rappuoli, R., Lanzavecchia, A., 2004. An efficient method to make human monoclonal antibodies from memory B cells: potent neutralization of SARS coronavirus. Nat. Med. 10, 871–875.
VanBlargan, L.A., Errico, J.M., Halfmann, P.J., Zost, S.J., Crowe Jr., J.E., Purcell, L.A., Kawaoka, Y., Corti, D., Fremont, D.H., Diamond, M.S., 2022. An infectious SARS-CoV-2 B.1.1.529 Omicron virus escapes neutralization by therapeutic monoclonal antibodies. Nat. Med. 28, 490–495.
Wang, Q., Michailidis, E., Yu, Y., Wang, Z., Hurley, A.M., Oren, D.A., Mayer, C.T., Gazumyan, A., Liu, Z., Zhou, Y., Schoofs, T., Yao, K.H., Nieke, J.P., Wu, J., Jiang, Q., Zou, C., Kabbani, M., Quirk, C., Oliveira, T., Chhosphel, K., Zhang, Q., Schneider, W. M., Jahan, C., Ying, T., Horowitz, J., Caskey, M., Jankovic, M., Robbiani, D.F., Wen, Y., de Jong, Y.P., Rice, C.M., Nussenzweig, M.C., 2020. A combination of human broadly neutralizing antibodies against hepatitis B virus HBsAg with distinct epitopes suppresses escape mutations. Cell Host Microbe 28, 335–349.e6.
Wec, A.Z., Wrapp, D., Herbert, A.S., Maurer, D.P., Haslwanter, D., Sakharkar, M., Jangra, R.K., Dieterle, M.E., Lilov, A., Huang, D., Tse, L.V., Johnson, N.V., Hsieh, C. L., Wang, N., Nett, J.H., Champney, E., Burnina, I., Brown, M., Lin, S., Sinclair, M., Johnson, C., Pudi, S., Bortz 3rd, R., Wirchnianski, A.S., Laudermilch, E., Florez, C., Fels, J.M., O'Brien, C.M., Graham, B.S., Nemazee, D., Burton, D.R., Baric, R.S., Voss, J.E., Chandran, K., Dye, J.M., McLellan, J.S., Walker, L.M., 2020. Broad neutralization of SARS-related viruses by human monoclonal antibodies. Science 369, 731–736.
Weinreich, D.M., Sivapalasingam, S., Norton, T., Ali, S., Gao, H., Bhore, R., Xiao, J., Hooper, A.T., Hamilton, J.D., Musser, B.J., Rofail, D., Hussein, M., Im, J., Atmodjo, D.Y., Perry, C., Pan, C., Mahmood, A., Hosain, R., Davis, J.D., Turner, K.C., Baum, A., Kyratsous, C.A., Kim, Y., Cook, A., Kampman, W., Roque-Guerrero, L., Acloque, G., Aazami, H., Cannon, K., Simon-Campos, J.A., Bocchini, J.A., Kowal, B., DiCioccio, A.T., Soo, Y., Geba, G.P., Stahl, N., Lipsich, L., Braunstein, N., Herman, G., Yancopoulos, G.D., Trial, Investigators, 2021. REGEN-COV antibody combination and outcomes in outpatients with covid-19. N. Engl. J. Med. 385, e81.
WHO, 2020. Clinical Management of COVID-19: Interim Guidance. WHO. https://apps.who.int/iris/handle/10665/332196. (Accessed 28 January 2022).
WHO Coronavirus. (COVID-19) dashboard. https://covid19.who.int/. (Accessed 28 January 2022).
Wrammert, J., Koutsonanos, D., Li, G.M., Edupuganti, S., Sui, J., Morrissey, M., McCausland, M., Skountzou, I., Hornig, M., Lipkin, W.I., Mehta, A., Razavi, B., Del Rio, C., Zheng, N.Y., Lee, J.H., Huang, M., Ali, Z., Kaur, K., Andrews, S., Amara, R.R., Wang, Y., Das, S.R., O'Donnell, C.D., Yewdell, J.W., Subbarao, K., Marasco, W.A., Mulligan, M.J., Compans, R., Ahmed, R., Wilson, P.C., 2011. Broadly cross-reactive antibodies dominate the human B cell response against 2009 pandemic H1N1 influenza virus infection. J. Exp. Med. 208, 181–193.
Wu, N.C., Yuan, M., Liu, H., Lee, C.D., Zhu, X., Bangaru, S., Torres, J.L., Caniels, T.G., Brouwer, P.J.M., van Gils, M.J., Sanders, R.W., Ward, A.B., Wilson, I.A., 2020a. An alternative binding mode of IGHV3-53 antibodies to the SARS-CoV-2 receptor binding domain. Cell Rep 33, 108274.
Wu, Y., Li, C., Xia, S., Tian, X., Kong, Y., Wang, Z., Gu, C., Zhang, R., Tu, C., Xie, Y., Yang, Z., Lu, L., Jiang, S., Ying, T., 2020b. Identification of human single-domain antibodies against SARS-CoV-2. Cell Host Microbe 27, 891-898.e5.
Yuan, M., Liu, H., Wu, N.C., Lee, C.D., Zhu, X., Zhao, F., Huang, D., Yu, W., Hua, Y., Tien, H., Rogers, T.F., Landais, E., Sok, D., Jardine, J.G., Burton, D.R., Wilson, I.A., 2020. Structural basis of a shared antibody response to SARS-CoV-2. Science 369, 1119–1123.
Zost, S.J., Gilchuk, P., Case, J.B., Binshtein, E., Chen, R.E., Nkolola, J.P., Schafer, A., Reidy, J.X., Trivette, A., Nargi, R.S., Sutton, R.E., Suryadevara, N., Martinez, D.R., Williamson, L.E., Chen, E.C., Jones, T., Day, S., Myers, L., Hassan, A.O., Kafai, N.M., Winkler, E.S., Fox, J.M., Shrihari, S., Mueller, B.K., Meiler, J., Chandrashekar, A., Mercado, N.B., Steinhardt, J.J., Ren, K., Loo, Y.M., Kallewaard, N.L., McCune, B.T., Keeler, S.P., Holtzman, M.J., Barouch, D.H., Gralinski, L.E., Baric, R.S., Thackray, L. B., Diamond, M.S., Carnahan, R.H., Crowe Jr., J.E., 2020. Potently neutralizing and protective human antibodies against SARS-CoV-2. Nature 584, 443–449.